Surface Nuclear Magnetic Resonance Imaging of Large Systems

Peter B. Weichman,[1] Eugene M. Lavely,[1] and Michael H. Ritzwoller[2]

[1]*Blackhawk Geometrics, Suite B, 301 Commercial Road, Golden, Colorado 80401*
[2]*Department of Physics, University of Colorado at Boulder, Boulder, Colorado 80309-0390*
(Received 17 December 1998)

The general theory of surface NMR imaging of large electromagnetically active systems is considered, motivated by geophysical applications. A general imaging equation is derived for the NMR voltage response, valid for arbitrary transmitter and receiver loop geometry and arbitrary conductivity structure of the sample. When the conductivity grows to the point where the electromagnetic skin depth becomes comparable to the sample size, significant diffusive retardation effects occur that strongly affect the signal. Accounting for these now allows more accurate imaging than previously possible. It is shown that the time constant T_1 may in principle be inferred directly from the diffusive tail of the signal. [S0031-9007(99)09154-1]

The nuclear magnetic resonance (NMR) technique provides a method for measuring the nuclear magnetic moment of a sample in a static magnetic field $\mathbf{B}_0$. The nuclear spins are pulsed with an ac magnetic field that is tuned to oscillate at the Larmor frequency $\omega_L \equiv 2\pi\nu_L = \gamma B_0$, where γ (= 4258 Hz/G for a free proton) is the gyromagnetic ratio. This causes the spins to tip away from and then precess about $\mathbf{B}_0$ at frequency ω_L. The ac voltage generated in the NMR receiver loop by the precessing spins then may be used to determine the original nuclear magnetic moment [1]. Free induction decay characteristics of the signal also carry information about inhomogeneities in $\mathbf{B}_0$ and microscopic interactions.

In many applications it is only part of the sample, e.g., hydrogen nuclei in water or in certain organic molecules, that contains free (i.e., unpinned by internal fields) nuclear spins, and it is of interest to obtain a spatially resolved image of this active region. There are two common ways of doing this. The first, used, e.g., in medical imaging, is to apply a small linear gradient to the static field. The Larmor frequency then varies in space, and only on some surface does it match the frequency of the ac field. Only spins close to this surface will then be tipped and contribute to the voltage signal. By varying the field gradient and the ac frequency different regions of the sample are resolved, and by performing an appropriate transform on these variables, the position dependent nuclear spin number density $n_N(\mathbf{r})$ is obtained.

In the second technique [2], known as surface NMR (or rotating frame imaging, using surface coils, in medicine), the placement of the transmitter loop that generates the ac field is geometrically limited, e.g., by physical or economic considerations. Such is the case in geophysical applications where the NMR apparatus is confined to the earth's surface or inside a bore hole. The ac field then has a nontrivial spatial distribution, and spins will be tipped by different angles at different points in space. Controlled gradients in the applied field are then impossible as well,

and imaging may be accomplished only by varying the pulse length τ_p and the relative sample position $\mathbf{x}_0$. The inverse problem to obtain $n_N(\mathbf{r})$ then becomes highly nontrivial [3,4], and uniformity of $\mathbf{B}_0$ is greatly desirable. In geophysical applications this is accomplished by using the earth's field as $\mathbf{B}_0$.

In typical laboratory (nongeophysical) applications, experimental parameters are chosen so that the transmitted and received magnetic fields are at most weakly perturbed by the bulk electromagnetic properties of the sample. Generally this requirement places an upper bound on the Larmor frequency, and hence on the magnitude of the static field $\mathbf{B}_0$ itself. The NMR signal is directly proportional to the equilibrium nuclear magnetization $\mathbf{M}_N^{(0)}(\mathbf{r}) = \chi_N(T)n_N(\mathbf{r})\mathbf{B}_0$, where χ_N is the single spin static susceptibility [5], which increases with the static field, and an upper bound is then also placed on the measurement sensitivity.

In certain geophysical applications, such as groundwater exploration [3,4], one has a complementary problem. The active volume is roughly the same size $L = 50–100$ m as the transmitter loop. The proton Larmor frequency in the earth's field is about 2 kHz, and the skin depth δ_s at this frequency falls into range L or less for ground resistivities below about 10 Ω m. The latter typically vary from 2 Ω m for very salty soils to 50 Ω m for clean soils. Quantitative analysis of data from depths of order δ_s then requires that one account for the distortion effects of the ground on the electromagnetic signal propagating to and from the nuclear spins.

We present in this Letter a quantitative theory that fully accounts for the effects of sample conductivity, assumed known or inferred from other measurements, on the measured NMR signal. We consider here only the case of uniform $\mathbf{B}_0$ [6]. The resulting imaging equation, (15) and (16) below, has quite a remarkable structure, is quite different from any used previously in the literature, and will have a significant impact on the interpretation of a number of experiments [3].

Let $\mathbf{B}_T(\mathbf{r}, t)$ be the ac transmitter loop field, and let $\mathbf{B}_N(\mathbf{r}, t) = \nabla \times \mathbf{A}_N(\mathbf{r}, t)$ be the field, and associated vector potential, generated by the nuclear spins [7]. The corresponding receiver loop voltage (in Gaussian units, which are used throughout unless explicitly stated otherwise) is then $V(t) = -(1/c)\, d\Phi(t)/dt$, where

$$\Phi(t) = \int_S \mathbf{B}_N(\mathbf{r}, t) \cdot \hat{\mathbf{n}}\, dA = \int_C \mathbf{A}_N(\mathbf{r}, t) \cdot d\mathbf{l} \quad (1)$$

is the magnetic flux through any surface S spanning the receiver loop C. Let this loop be parametrized by a curve $\vec{\gamma}(s)$, $0 \leq s < l$, with $\vec{\gamma}(0) = \vec{\gamma}(l)$. It is convenient to define a fictitious current density,

$$J_R(\mathbf{r}) = \int_0^l ds\, \partial_s \vec{\gamma}_R(s) \delta[\mathbf{r} - \vec{\gamma}_R(s)], \quad (2)$$

living on the curve C. A current I in the receiver loop would yield a physical current density $I J_R$. The flux may then be written in the form

$$\Phi(t) = \int d^3 r\, \mathbf{A}_N(\mathbf{r}, t) \cdot J_R(\mathbf{r}). \quad (3)$$

Choosing a gauge in which the static potential vanishes, $\mathbf{A}_N$ satisfies the frequency domain equation

$$\nabla \times \left(\frac{1}{\mu} \nabla \times \mathbf{A}_N \right) - \epsilon k^2 \mathbf{A}_N = \frac{4\pi}{c}\, \mathbf{j}_N, \quad (4)$$

where $k = \omega/c$, and $\mathbf{j}_N = c\nabla \times \mathbf{M}_N$ is the microscopic current density associated with $\mathbf{M}_N$. The frequency dependent dielectric function has the low frequency form $\epsilon(\mathbf{r}, \omega) = 4\pi i \sigma/\omega$, where $\sigma(\mathbf{r})$ is the local dc conductivity. The magnetic permeability μ is also in general frequency and position dependent. Now, let $\mathcal{A}_R$ be defined to satisfy (4) with $J_R(\mathbf{r})$ replacing $\mathbf{j}_N$. Even though J_R is frequency independent, $\mathcal{A}_R(\mathbf{r}, \omega)$ will gain frequency dependence from ϵ and μ. The inverse Fourier transform of (4) then shows that $\mathcal{A}_R(\mathbf{r}, t)$ is the field produced by a delta-function current pulse $J_R(\mathbf{r})\delta(t)$ in the receiver loop. Causality requires that $\mathcal{A}_R(\mathbf{r}, t)$ vanish for $t < 0$. Substituting the equation for $\mathcal{A}_R$ into (3) and integrating by parts, one obtains

$$\Phi(t) = \int d^3 r \int_0^\infty dt'\, \mathbf{j}_N(\mathbf{r}, t - t') \cdot \mathcal{A}_R(\mathbf{r}, t'), \quad (5)$$

representing a kind of reciprocity theorem. Finally, substituting the nuclear magnetization and integrating by parts one more time, one obtains for the voltage

$$V(t) = -\int d^3 r \int_0^\infty dt'\, \mathcal{B}_R(\mathbf{r}, t') \cdot \partial_t \mathbf{M}_N(\mathbf{r}, t - t'), \quad (6)$$

where $\mathcal{B}_R = \nabla \times \mathcal{A}_R$ is the fictitious magnetic field due to the delta-function pulse in the receiver loop.

The field $\mathcal{B}_R$ encodes the sensitivity of the receiver loop to $\mathbf{M}_N(\mathbf{r}, t)$ at a particular space-time point, and its t' dependence encodes delay effects due to the transit time of the signal from $\mathbf{r}$ to the receiver loop. At low frequencies this delay is dominated by diffusive, not speed of light, effects. Thus, e.g., with $\mu = 1$ and $\epsilon = 4\pi i \sigma/\omega$, Eq. (4) is the diffusion equation with diffusion constant $D = c^2/4\pi\sigma$. The delay time over the sample size L will then scale as $\tau_d \sim L^2/D$. Since the skin depth is given by $\delta_s = \sqrt{2D/\omega}$, one has $\omega_L \tau_d \sim L^2/\delta_s(\omega_L)^2$. Thus if $\mathbf{M}_N$ has dynamics on the time scale $\tau_L = 1/\nu_L$ of the Larmor period, the t' integral weighted by $\mathcal{B}_R$ in (6) will result in significant time averaging of the dynamics of $\mathbf{M}_N$ when $\delta_s(\omega_L)/L = O(1)$. In MKS units appropriate to the geophysical problem, one has

$$\omega_L \tau_d = 2\pi^2 \left(\frac{\nu_L}{1\,\text{kHz}} \right) \left(\frac{L}{100\,\text{m}} \right)^2 \left(\frac{1\,\Omega\,\text{m}}{\rho} \right), \quad (7)$$

where $\rho = 1/\sigma$ is the resistivity. The earlier estimates follow from this formula. On the other hand, in the *adiabatic limit* $L \ll \delta_s(\omega_L)$, where $\mathbf{M}_N$ varies slowly on the scale of τ_d, Eq. (6) reduces to

$$V(t) = -\int d^3 r\, \mathcal{B}_R^0(\mathbf{r}) \cdot \partial_t \mathbf{M}_N(\mathbf{r}, t), \quad (8)$$

in which $\mathcal{B}_R^0(\mathbf{r}) = \int_0^\infty dt\, \mathcal{B}_R(\mathbf{r}, t)$ is the *static* field generated by a *steady* current J_R in the receiver loop.

During the tipping pulse, $0 \leq t \leq \tau_p$, the transmitter loop current is given by $I_T(t) = I_T^0 \cos(\omega_L t)$. We assume $\tau_p \gg \tau_d$ so that after a brief transient the transmitted field will also be periodic with frequency ω_L. It is the *corotating part* of $\mathbf{B}_T^\perp = \mathbf{B}_T - (\hat{\mathbf{B}}_0 \cdot \mathbf{B}_T)\hat{\mathbf{B}}_0$ (the projection of the transmitted field into the plane orthogonal to $\mathbf{B}_0$) that tips the spins away from $\mathbf{B}_0$. Thus $\mathbf{B}_T^\perp$ is in general elliptically polarized, but may be decomposed into clockwise corotating and counterclockwise counterrotating circularly polarized components: $\mathbf{B}_T^\perp = \mathbf{B}_T^+ + \mathbf{B}_T^-$. One may write [8]

$$\mathbf{B}_T^\pm = I_T^0 \rho_T^\pm [\cos(\omega_L t - \zeta_T)\hat{\mathbf{b}}_T \\ \mp \sin(\omega_L t - \zeta_T)\hat{\mathbf{B}}_0 \times \hat{\mathbf{b}}_T], \quad (9)$$

in which $\hat{\mathbf{b}}_T(\mathbf{r}, \omega_L)$ is the semimajor axis of the ellipse, $I_T^0 \rho_T^\pm(\mathbf{r}, \omega_L) = |\mathbf{B}_T^\pm|$ are the magnitudes of the two circular components, and $\zeta_T(\mathbf{r}, \omega_L)$ is the *phase delay* (due to diffusive retardation) between the transmitter current and $\mathbf{B}_T^\perp$. For $0 \leq t < \tau_p$ one then finds

$$\mathbf{M}_N(\mathbf{r}, t) = \mathbf{M}_N^{(0)} \cos(\omega_T t) + \mathbf{M}_N^{(0)} \times \hat{\mathbf{B}}_T^+ \sin(\omega_T t), \quad (10)$$

in which $\hat{\mathbf{B}}_T^+$ is a unit vector along $\mathbf{B}_T^+(\mathbf{r})$, and $\omega_T(\mathbf{r}) = \gamma|\mathbf{B}_T^+|$. Equation (10) represents the standard solution to the free spin Bloch dynamics in which, in the frame corotating with $\mathbf{B}_T^+$, $\mathbf{M}_N$ rotates clockwise about $\mathbf{B}_T^+$ at rate ω_T [1]. For $t > \tau_p$ the spins continue to precess at a fixed tipping angle $\theta_T = \omega_T \tau_p$, but dissipation and dephasing effects will also cause slow reequilibration. This is accounted for phenomenologically with time constants $T_1(\mathbf{r})$ and $T_2(\mathbf{r})$ describing, respectively, the recovery of

the magnetization along $\mathbf{B}_0$, and the decay of the precessing in-plane magnetization:

$$\mathbf{M}_N(\mathbf{r}, t) = \mathbf{M}_N^{(0)}\{1 + e^{-(t-\tau_p)/T_1}[\cos(\omega_T\tau_p) - 1]\}$$
$$+ e^{-(t-\tau_p)/T_2}\mathbf{M}_N^{(0)} \times \hat{\mathbf{B}}_T^+ \sin(\omega_T\tau_p), \quad (11)$$

in which $\hat{\mathbf{B}}_T^+$ continues to be defined by (9) for $t > \tau_p$. Under the assumption that $\omega_L/\omega_T, \omega_L T_1, \omega_L T_2 \gg 1$, the time derivative of the magnetization is dominated by the Larmor precession, and one obtains

$$\partial_t\mathbf{M}_N = \omega_L M_N^{(0)} e^{-(t-\tau_p)/T_2} \sin(\omega_T\tau_p)\hat{\mathbf{B}}_T^+. \quad (12)$$

Substituting (12) into (6) one obtains

$$V(t) = -\frac{\omega_L}{2} \int d^3r\, M_N^{(0)} \sin(\omega_T\tau_p)e^{-(t-\tau_p)/T_2}$$
$$\times \{e^{-i(\omega_L t-\zeta_T)}(\hat{\mathbf{b}}_T - i\hat{\mathbf{B}}_0 \times \hat{\mathbf{b}}_T) \cdot \int_0^{t_{\max}} dt'$$
$$\times e^{(i\omega_L+1/T_2)t'}\mathcal{B}_R(\mathbf{r}, t') + c.c.\}, \quad (13)$$

where c.c. stands for complex conjugate, and the upper limit $t - \tau_p < t_{\max} < t$ stands as a reminder that (12) is valid only for $t > \tau_p$ and that the signal vanishes identically for $t < 0$. This cutoff is important at large times because the delay function $\mathcal{B}_R(\mathbf{r}, t') \approx \tau_d^{-1}\mathcal{B}_\infty(\mathbf{r})(\tau_d/t')^p$ decays as a power law $p = 5/2$ at large times (see below). The e^{t'/T_2} factor then dominates at large time and the response is determined by the cutoff. The signal is then determined by the late arrival of the diffusive tail of the field that was generated at early times. This effect will be considered quantitatively below. Of primary interest, however, is the NMR signal at early times, $\tau_p + \tau_d \ll t \ll T_1, T_2$. In this regime one may drop the exponential decay factors. The cutoff is no longer needed for convergence and one obtains $V(t) = \mathrm{Re}\,V_0 e^{-i\omega_L t}$ with complex amplitude

$$V_0 = -\omega_L \int d^3r\, M_N^{(0)} \sin(\omega_T\tau_p)e^{i\zeta_T}$$
$$\times \mathcal{B}_R(\mathbf{r}, \omega_L) \cdot (\hat{\mathbf{b}}_T - i\hat{\mathbf{B}}_0 \times \hat{\mathbf{b}}_T). \quad (14)$$

It is therefore only the Larmor frequency Fourier component of $\mathcal{B}_R(\mathbf{r}, t)$ that enters the early time signal. It is, in fact, (the real and imaginary parts of) V_0 that are output directly from the standard NMR quadrature detection scheme [1]. To put (14) into a more convenient form, decompose the in-plane projection of $\mathcal{B}_R(\mathbf{r}, \omega_L)$ in the form (9) with corresponding parameters $\rho_R^\pm$, ζ_R, and $\hat{\mathbf{b}}_R$. Substituting the result into (14) one obtains finally the fundamental imaging equation

$$V_0(q, \mathbf{x}_0) = \int d^3r\, K(q, \mathbf{x}_0; \mathbf{r})n_N(\mathbf{r}) \quad (15)$$

in which we have now explicitly displayed the experimentally controllable *pulse moment* $q \equiv I_T^0\tau_p$, and sample position $\mathbf{x}_0$, relative to the transmitter and receiver

loops. The kernel is given by

$$K(q, \mathbf{x}_0; \mathbf{r}) = -2\omega_L\chi_N B_0 e^{i(\zeta_T+\zeta_R)}\rho_R^- \sin(\gamma q\rho_T^+)$$
$$\times (\hat{\mathbf{b}}_R \cdot \hat{\mathbf{b}}_T + i\hat{\mathbf{B}}_0 \cdot \hat{\mathbf{b}}_R \times \hat{\mathbf{b}}_T). \quad (16)$$

Equations (15) and (16) are our basic results. The factor ρ_R^- indicates that it is the counterrotating part of the receiver loop field that enters K. This is due to the fact that the latter enters as a memory effect, i.e., in a time reversed fashion. The phase factor $e^{i(\zeta_R+\zeta_T)}$ shows that phase delay effects arise from the propagation of the transmitted signal both to and from the sample. In many applications the receiver and transmitter loops coincide, the voltage measurement being made only a suitable delay time after the end of the tipping pulse. In this case one may simplify (16) to the form

$$K(q, \mathbf{x}_0; \mathbf{r}) = -\frac{2\omega_L\chi_N B_0}{I_T^0} e^{2i\zeta_T}|\mathbf{B}_T^-| \sin(\gamma\tau_p|\mathbf{B}_T^+|). \quad (17)$$

Kernels resembling (17) have been used in the geophysical literature [3,4,9], but the distinction between $\mathbf{B}_T^+$ and $\mathbf{B}_T^-$, and the presence of the crucial phase factor ζ_T has not been previously recognized. Previous kernels either implicitly assumed the validity of the adiabatic limit, where $\zeta_T = 0$ and $|\mathbf{B}_T^+| = |\mathbf{B}_T^-|$ are both exactly half the amplitude of the total transmitted signal, or were based on naive incorrect generalizations of this limit.

Consider now an application to a geophysically motivated imaging problem. Let the ground have uniform conductivity $\sigma = 0.05$ S/m, yielding a skin depth $\delta_s \simeq 50$ m at the Larmor frequency corresponding to the earth's field, and a single unbounded horizontal layer of saturated water of various thicknesses placed at various depths: 10–20, 30–45, and 60–80 m. In the left-hand side of Fig. 1 we plot the complex NMR voltage amplitude calculated from (17) for coincident 100 m diameter circular transmitter and receiver loops over a range of q designed to significantly tip spins as deep as 100 m. Notice that the largest response occurs at larger q as the depth of the water layer increases. In the right-hand side of Fig. 1 we show the results of inverting the conducting voltage data using (i) both real and imaginary parts of the data, (ii) only the real part of the data, and (iii) only the real part of the data along with the (incorrect) insulating kernel. The inversion accuracy progressively degrades, with (iii) even predicting dominantly negative water content in the case of the deepest layer. Only (i) provides an accurate reconstruction. This exercise demonstrates convincingly that even *qualitatively* correct inversions at depths comparable to δ_s require the new theory.

Finally, consider the decay characteristics of the NMR signal. From (13) it follows that the ω_L Fourier component of the signal is obtained simply by multiplying the kernel K by $e^{-(t-\tau_p)/T_2(\mathbf{r})}$. The later time signal, $t/T_2 = O(1)$, is then a linear superposition of exponential decays reflecting strengths of the various dephasing
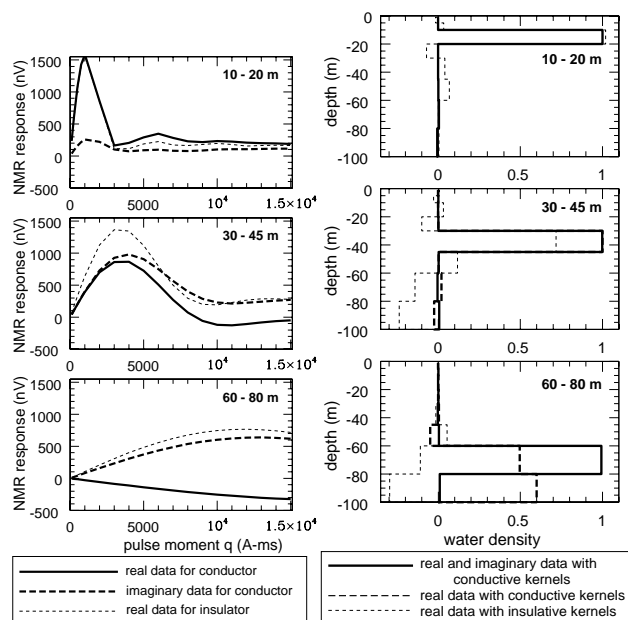
FIG. 1. Model geophysical application to detection of a layer of saturated water of various widths at various depths (shown in each panel). Left: Calculated complex NMR voltage amplitude for conducting ($\sigma = 0.05$ S/m) and insulating subsurface half spaces. Right: Recovery of the original water distribution by inversion of the conducting data on the left. Note the large degradation in the accuracy of the inversion, including unphysically negative water content, when the imaginary part of the voltage is not used, and when the incorrect insulating kernel is used.

processes throughout the sample. This is, in fact, the basis for T_1 and T_2 contrast imaging in medical applications. In the application to imaging water in porous rock, $1/T_2 \propto n_{\mathrm{imp}} S/V$, where n_{imp} is the density of paramagnetic impurities on the pore surfaces and S/V is their surface-to-volume ratio [10]. If one uses the early time data to invert (15) for $n_N(\mathbf{r})$, the later time data may then be inverted to give information about the pore size distribution. The latter directly reflects the diffusivity of the fluid through the rock and is crucial, e.g., in oil recovery and toxic contaminant containment.

At very late times, $t \gg T_1, T_2$, the Larmor Fourier component disappears and the overall signal becomes dominated by the upper cutoff $t_{\max}$ in (13). In this limit $\mathcal{B}_R$ varies slowly on the scales of T_1 and T_2, and one may factor it out of the time integral. Starting from the original form (6), one obtains then the decaying dc signal

$$V(t) \approx \frac{p}{\tau_d^2}\left(\frac{\tau_d}{t}\right)^{p+1} \int d^3 r\, \mathcal{B}_\infty(\mathbf{r}) \cdot \mathcal{M}_N(\mathbf{r}), \quad (18)$$

in which $\mathcal{M}_N = \int_{-\infty}^{\infty} ds\,[\mathbf{M}(\mathbf{r},s) - \mathbf{M}_N^{(0)}(\mathbf{r})]$ is the total integrated *magnetization pulse,* and $\mathcal{B}_\infty$ was introduced below (13). Since the in-plane magnetization oscillates

rapidly, it averages essentially to zero and makes a negligible contribution to $\mathcal{M}_N$. The main contribution then comes from the T_1 decay of the parallel magnetization that was neglected in (12). Using (10) and (11), and assuming that $T_1 \gg \tau_p$, as is typically the case, one obtains

$$\mathcal{M}_N \approx -\mathbf{M}_N^{(0)}[1 - \cos(\omega_T \tau_p)]T_1. \quad (19)$$

The amplitude of the decaying signal (18) then directly reflects the distribution of time constants T_1, which in laboratory measurements are obtained by pulsing the static field [1]. Unfortunately, since $T_2 \gg \tau_d$ by 3 orders of magnitude or more, the power law prefactor in (18) is extremely small, and this amplitude will be very difficult to extract.

In conclusion, Eqs. (15)–(17) provide explicit, compact forms for analyzing NMR data in the presence of a known electromagnetically active environment. Recent and planned geophysical measurements fall into a regime where accounting for environmental conductivity effects is crucial. In future work [11] the corresponding inverse problem will be analyzed in greater detail and quantitatively compared to experimental data.

[1] See, e.g., A. Abragam, *Principles of Nuclear Magnetism* (Oxford University Press, New York, 1983).

[2] See, e.g., D. I. Hoult and R. E. Richards, J. Magn. Reson. **24**, 71 (1976).

[3] See, e.g., D. V. Trushkin, O. A. Shushakov, and A. V. Legchenko, Geophys. Prospect. **43**, 623 (1995).

[4] A. V. Legchenko and O. A. Shushakov, Geophysics **63**, 75 (1998).

[5] For noninteracting spins, the Curie law [1] $\chi_N = \gamma^2 \hbar^2 J(J+1)/3k_B T$ is appropriate, where J is the nuclear spin.

[6] A combined theory accounting for nonuniformities in both $\mathbf{B}_0$ and the ac field, essentially merging the two imaging methods, will be considered in later work. This theory would probably be most useful for enhancing the resolution of the first method by correcting for small nonuniformities in the ac field.

[7] All fields considered in this Letter are to be computed within the environment defined by ϵ and μ in (4).

[8] Computation of $\mathbf{B}_T^{\pm}$, with associated ζ_T, $\rho_T^{\pm}$, and $\hat{\mathbf{b}}_T$, from $\mathbf{B}_T^{\perp}$ is elementary. Details may be found in [11].

[9] M. Goldman, B. Rabinovich, M. Rabinovich, D. Gilad, I. Gev, and M. Schirov, J. Appl. Geophys. **31**, 27 (1994).

[10] R. L. Kleinberg, W. E. Kenyon, and P. P. Mitra, J. Magn. Reson. A **108**, 206 (1994).

[11] P. B. Weichman, E. L. Lavely, and M. Ritzwoller (unpublished).